



UNIVERSITY OF LEEDS

This is a repository copy of *Transport-controlled hydrothermal replacement of calcite by Mg-carbonates*.

White Rose Research Online URL for this paper:  
<http://eprints.whiterose.ac.uk/87655/>

Version: Accepted Version

---

**Article:**

Jonas, L, Mueller, T, Dohmen, R et al. (2 more authors) (2015) Transport-controlled hydrothermal replacement of calcite by Mg-carbonates. *Geology*, 43 (9). pp. 779-782. ISSN 0091-7613

<https://doi.org/10.1130/G36934.1>

---

**Reuse**

Unless indicated otherwise, fulltext items are protected by copyright with all rights reserved. The copyright exception in section 29 of the Copyright, Designs and Patents Act 1988 allows the making of a single copy solely for the purpose of non-commercial research or private study within the limits of fair dealing. The publisher or other rights-holder may allow further reproduction and re-use of this version - refer to the White Rose Research Online record for this item. Where records identify the publisher as the copyright holder, users can verify any specific terms of use on the publisher's website.

**Takedown**

If you consider content in White Rose Research Online to be in breach of UK law, please notify us by emailing [eprints@whiterose.ac.uk](mailto:eprints@whiterose.ac.uk) including the URL of the record and the reason for the withdrawal request.



[eprints@whiterose.ac.uk](mailto:eprints@whiterose.ac.uk)  
<https://eprints.whiterose.ac.uk/>

1 Transport-controlled hydrothermal replacement of calcite  
2 by Mg carbonates

3 **Laura Jonas<sup>1\*</sup>, Thomas Müller<sup>1,\*2</sup>, Ralf Dohmen<sup>1\*</sup>, Lukas Baumgartner<sup>3\*</sup>, and**  
4 **Benita Putlitz<sup>3\*</sup>**

5 *<sup>1</sup>Institut für Geologie, Mineralogie und Geophysik, Ruhr-Universität Bochum,*

6 *<sup>2</sup>School of Earth and Environmental Sciences, University of Leeds, LS2 9JT Leeds, UK*

7 *Universitätsstrasse 150, D-44801 Bochum, Germany*

8 *<sup>3</sup>Institute of Earth Sciences, University of Lausanne, Geopolis Building, CH-1015*

9 *Lausanne, Switzerland*

10 \*E-mails: laura.jonas@rub.de; ralf.dohmen@rub.de; t.mueller@leeds.ac.uk;

11 lukas.baumgartner@unil.ch; benita.putlitz@unil.ch.

12 **ABSTRACT**

13 Dolomitization is one of the most important diagenetic processes but the reaction  
14 rate and timescale of dolomitization remain a topic of controversy. We conducted  
15 experiments in which the reaction of single calcite crystals with a Mg-rich fluid at 200 °C  
16 leads to the formation of a zoned reaction rim consisting of magnesite and for  
17 intermediate times Ca-rich dolomite. From detailed documentation of the evolution of the  
18 microtexture and chemical composition of the reaction rim we infer a kinetic model for  
19 calcite replacement by Mg-carbonates. The chemical gradient for the structure forming  
20 elements Mg and Ca in the reaction rim and the evolution of the rim thickness strongly  
21 indicate that the overall reaction rate is controlled by diffusive transport through the  
22 porous reaction rim. The composition of the product phases is kinetically controlled and

23 records the local composition of the interfacial fluid without requiring oversaturation of  
24 the reservoir fluid. Reactive transport models on dolomitization processes assume that the  
25 rate of dolomitization depends on the rate of dolomite precipitation, which is  
26 contradictory to our experimental evidence. Modeling carbonate replacement in natural  
27 systems requires detailed knowledge on the evolution of the microstructure controlling  
28 the physicochemical transport properties of elements in the pore fluid.

## 29 **INTRODUCTION**

30 Dolomites comprise a large fraction of oil and gas reservoir rocks and are of  
31 substantial economic importance. The formation of dolomite is commonly considered to  
32 take place by the replacement of a precursor limestone. Reactive transport models are  
33 used to predict the rates and spatial patterns of dolomitization (e.g., Wilson et al., 2001;  
34 Jones and Xiao, 2005; Whitaker and Xiao, 2010) and apply data from dolomite  
35 precipitation experiments (e.g., Arvidson and Mackenzie, 1999) to calculate the overall  
36 reaction rate. The replacement reaction consists of a series of processes including  
37 dissolution, transport and precipitation (e.g., Mueller et al., 2010, and references therein).  
38 The use of precipitation rates is only justified if precipitation is the slowest and thus rate  
39 limiting process, which is not yet experimentally proven.

40 Hydrothermal carbonate-carbonate replacement experiments were carried out to  
41 investigate the stability fields in different carbonate-fluid systems with saline solutions of  
42 different composition. Most of these studies used saline solutions to react with powdered  
43 carbonate materials with high reactive surface to solid volume ratios (e.g., Graf and  
44 Goldsmith, 1955; Katz and Matthews, 1977; Kaczmarek and Sibley, 2011).

45 Hydrothermal experiments on replacement of fragments of recent and fossil  
46 biogenic carbonates by dolomite (e.g., Bullen and Sibley, 1984; Grover and Kubanek,  
47 1983) and single aragonite crystals by calcite (e.g., Perdikouri et al., 2011) were  
48 conducted. Since many studies on carbonate replacement are based on experiments with  
49 powdered material, no detailed studies of the developing microstructures accompanying  
50 the replacement of single calcite crystals by Mg carbonates have been published to date.  
51 We present a series of hydrothermal experiments using single calcite crystals and Mg-  
52 rich fluid to gain understanding of the mechanisms and rates controlling the replacement.  
53 The use of single crystals with planar surfaces and homogeneous composition allows to  
54 study the evolving microstructures and to analyze the reaction product's chemical  
55 composition with high spatial resolution. Coupling information on the microstructures  
56 with chemical data and reaction rates enables a quantitative description of the element  
57 fluxes controlling the reaction progress. Our results demonstrate that element transport on  
58 the grain scale, rather than the precipitation rate, is controlling the local fluid chemistry,  
59 the precipitating phase and the transformation rate of an individual crystal. Identification  
60 of the rate-limiting step is crucial to develop a parameterization for the rate of  
61 dolomitization and its prediction in natural systems, e.g., for burial dolomitization in  
62 diagenetic environments.

### 63 **EXPERIMENTAL AND ANALYTICAL METHODS**

64 Single calcite crystals ( $\sim 2 \times 2 \times 2$  mm) were split using a razorblade and reacted  
65 with a 1 M  $\text{MgCl}_2$  solution prepared from anhydrous  $\text{MgCl}_2$  (Sigma-Aldrich Chemie  
66 GmbH,  $\geq 98\%$ ) and distilled water. In each experiment, one crystal and 1 mL of liquid  
67 were placed into a Teflon<sup>®</sup>-lined steel autoclave and reacted at 200 °C at vapor-saturated

68 conditions (~16 bars). Five experiments were performed with times of 1, 3, 7, 14, and 28  
69 days. After reaction, the autoclaves were removed from the furnace and cooled to room  
70 temperature in ~60 min. The fluid was removed from the reactors and analyzed using  
71 atomic absorption spectroscopy (AAS). The crystals were washed with distilled water  
72 and dried at ~120 °C for 30 min. Internal features were imaged using non-destructive  
73 computed X-Ray micro-tomography ( $\mu$ CT). The microstructures on the surface and  
74 within cross sections of reacted crystals were analyzed using scanning electron  
75 microscopy (SEM). The chemical composition was measured using electron microprobe  
76 analysis (EMPA). Details on all analytical methods used can be found in the GSA Data  
77 Repository<sup>1</sup>.

## 78 **RESULTS**

79 Mineral-fluid interaction causes the replacement of calcite by a Mg-carbonate  
80 phase, either magnesite and/or a Ca-Mg-carbonate with dolomitic composition (Fig. 1).  
81 The overall reaction is characterized by the formation of a porous, sometimes layered  
82 reaction rim that progresses continuously toward the center of the crystal. A remarkable  
83 microstructural characteristic is the formation of a gap separating the rim from the  
84 unreacted core, which is also visible in 3-D  $\mu$ CT images (Fig. 1B). The width of both the  
85 rim and the gap increases with time. The rim evolves through three stages (see Fig. DR2  
86 in the Data Repository). In the first stage, i.e., after 1–3 days, a thin magnesite layer  
87 replaces the outermost parts of the crystal. In experiments with intermediate run durations  
88 (~14 days), Ca-rich dolomite appears as a second product forming an intermediate layer  
89 between the calcite core and the magnesite rim. In the final stage (>28 days), only a thin  
90 layer of dolomite remains, and the rim consists almost solely of magnesite. Both the

91 overall size and shape of the parent crystal are preserved during the replacement. The  
92 polycrystalline reaction rim is built of small Mg-carbonate rhombs (see Fig. DR3). The  
93 whole reaction rim exhibits a non-homogeneously distributed porosity with a coarse  
94 porosity in the magnesite layer and a fine porosity in the dolomite layer. When magnesite  
95 replaces dolomite in later stages of the reaction, the newly formed magnesite “inherits”  
96 the fine porosity of the dolomite precursor.

97         The reaction rim has a complex geometry.  $\mu$ CT analysis show that the thickness  
98 of individual layers depends on the orientation and position of the respective cross  
99 section. Cross sections of the crystals prepared for SEM and EMPA reveal that the total  
100 fraction  $\zeta$ , i.e., the fraction of calcite transformed to Mg-carbonate, increases linearly  
101 with the square root of time.

102         The composition of the individual layers is not homogeneous. With increasing  
103 distance from the unreacted core the Mg concentrations increase while the amount of Ca  
104 decreases. These gradients are particularly pronounced in the magnesite layer (see Fig.  
105 DR1).

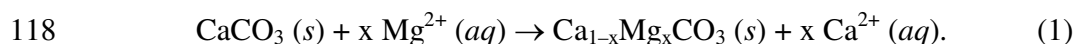
106         Continuous Mg-Ca exchange between mineral and fluid is also recorded by the  
107 time-dependent change in fluid composition. The bulk fluid is progressively enriched in  
108 Ca and depleted in Mg. The Ca/Mg ratio of the solution increases linearly with the square  
109 root of time (Fig. 2C).

## 110 **DISCUSSION**

### 111 **Microstructures and Reaction Mechanisms**

112  
113  
114

115 The exchange reaction between crystal and fluid involves the release of elements  
116 from the dissolving parent phase into the fluid and incorporation of elements from the  
117 fluid into the product phase:



119 The equation describes the dissolution of the solid (*s*) calcite that immediately  
120 reacts at the interface with an aqueous (*aq*)  $\text{Mg}^{2+}$  ion to precipitate Mg-carbonate.  
121 Simultaneously, a  $\text{Ca}^{2+}$  ion is released into the fluid. With increasing reaction progress,  
122 the fluid reservoir becomes enriched in Ca and depleted in Mg. Continuous reaction  
123 progress requires effective flux of Mg from the fluid reservoir through the reaction rim  
124 toward the reaction interface, countered by a flux of Ca in the opposite direction. The  
125 transport distance continuously increases with the growth of the rim (Fig. 3A). Both the  
126 observed sharp boundaries between the product layers and the core as well as the  
127 formation of small rhombs building the rim are characteristic of a dissolution-  
128 precipitation mechanism (see review of Putnis, 2009). The pseudomorphic replacement is  
129 accompanied by a maximum negative molar volume change ( $\Delta V$ ) of ~13% in the case of  
130 calcite being replaced by stoichiometric dolomite and ~23% for replacement by pure  
131 magnesite. The formation of interconnected porosity enables the reaction to progress  
132 further into the crystal (Putnis et al., 2005; Raufaste et al., 2011) and maintains the  
133 continuous element exchange between the fluid at the reaction interface and the fluid  
134 reservoir surrounding the crystal. However, the presence and size of the gap separating  
135 the rim from the unreacted calcite suggest that the gap comprises most of the volume  
136 loss. Some authors argue that the relative solubility of the phases contributes to the  
137 formation of porosity and the gap at the interface (e.g., Putnis, 2009). However, our

138 calculations show that only a minor amount of calcite needs to be dissolved to saturate  
139 the bulk fluid with magnesite and hence the gap is the result of the serial nature of the  
140 reaction in combination with the large negative molar volume change.

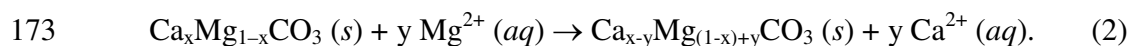
#### 141 **Kinetic Model**

142 The overall replacement comprises a serial process of dissolution, transport and  
143 precipitation, all of which proceed at different rates (e.g., Mueller et al. 2010). The net  
144 conversion rate is controlled by the slowest, rate-limiting step in this series of sub-  
145 processes. The rate of replacement and its controlling parameters can be inferred by the  
146 time-dependent data such as the thickness of the rim and the evolution of the pore fluid  
147 chemistry, which both approximately follow a parabolic rate law characteristic for a  
148 diffusion-controlled process (Fig. 2). Rim thickness varies significantly within each  
149 sample, which can be explained by local variation of the different fluxes due to limited  
150 accessibility to the fluid or the surfaces at the bottom of the crystal sitting on the capsule  
151 wall or 3-D effects for the diffusive flux at the crystal edges. The chemical gradient  
152 within each layer mirrors the flux of Mg toward the reaction interface, countered by the  
153 flux of Ca (Fig. 3A). The gradient in the solid reaction product is a proxy for the  
154 evolution of the fluid composition at the reaction interface as the reaction rim grows  
155 under local oversaturation with regard to the respective product phase.

156 In the first stages of the reaction, the Ca/Mg ratio in the fluid is still low and the  
157 removal of  $\text{Ca}^{2+}$  from the reaction interface is efficient enough to produce almost pure  
158 magnesite (Fig. 3B, stage 1). The width of the rim, i.e., the transport distance between the  
159 fluid reservoir and the fluid at the reaction interface, continuously increases and the  
160 removal of  $\text{Ca}^{2+}$  from the interface and the supply of  $\text{Mg}^{2+}$  from the reservoir toward the



161 interface become less efficient. Consequently, the Ca/Mg ratio in solution increases with  
162 increasing distance from the fluid reservoir. This leads to an increased incorporation of  
163  $\text{Ca}^{2+}$  into the magnesite that replaces calcite, i.e., the presence of a concentration gradient  
164 within the fluid causes the distinct compositional gradient within the product layer. At  
165 some point, the increasing Ca/Mg ratio in the interfacial fluid leads to supersaturation  
166 with respect to dolomite and facilitates dolomite nucleation. Thus a dolomite layer  
167 develops between the magnesite layer and the calcite (Fig. 3B, stage 2). In later stages of  
168 the replacement, the system approaches chemical equilibrium. Dissolution of calcite  
169 decelerates, whereas the concentration of Mg in the reservoir fluid is still high enough to  
170 supply the pore fluid with Mg. The fluid at the magnesite-dolomite interface becomes  
171 supersaturated with respect to Ca-bearing magnesite. This leads to the secondary  
172 replacement of dolomite by magnesite (Fig. 3B, stage 3):



174 At the final stage, the growth of magnesite is faster compared to dolomite, which  
175 must be related to a more efficient element transport within the magnesite layer.  
176 Enhanced porosity in the newly formed magnesite related to the volume change of  
177 Reaction 2 could be the reason since no gap formed at the magnesite-dolomite interface.

178 Therefore, we can explain our observations consistently assuming that the  
179 reaction is controlled by diffusion through the pore fluid. If one of the other serial  
180 processes (dissolution or precipitation) would be rate-limiting, the reaction could be  
181 classified as interface-controlled, but this would imply a homogeneous fluid composition  
182 throughout the reaction system (Lasaga, 1986). It is impossible to explain the appearance  
183 and disappearance of dolomite assuming a homogeneous but evolving fluid composition

184 since the observed Ca/Mg ratio in the fluid reservoir continuously increases and cannot  
185 explain sudden under-saturation with respect to dolomite in the later stage. When  
186 dolomite becomes undersaturated, the fluid at the magnesite-dolomite interface must  
187 have had a different composition compared to the fluid reservoir indicating gradients in  
188 the pore fluid.

189 We note, however, that most natural fluids contain higher Ca/Mg ratios than the  
190 reservoir fluid of our experiments. Thus, for natural dolomitization processes the  
191 formation of magnesite is likely omitted.

## 192 **IMPLICATIONS FOR OVERALL REACTION RATES OF DOLOMITIZATION**

193 Pseudomorphic replacement has been reported for other carbonate-carbonate  
194 replacements taking place by dissolution-precipitation (e.g., Grover and Kubanek, 1983;  
195 Bullen and Sibley, 1984; Perdikouri et al., 2011) and appears to be the most likely  
196 mechanism for dolomitization. Our experimental study illustrates the influence of fluid  
197 composition, i.e., the cation ratio in the reacting fluid, on the precipitating phase (either  
198 magnesite or dolomite) and its composition in agreement with previous studies (e.g.,  
199 Rosenberg et al., 1967; Sibley, 1990; Tribble et al., 1995; Kaczmarek and Sibley, 2011).  
200 However, to predict rates of dolomitization (or other carbonate replacements) an  
201 appropriate kinetic law needs to be formulated. Previous studies concluded that the rate  
202 of hydrothermal dolomitization increases with temperature, surface area, fluid-rock ratio,  
203 the concentration and Mg/Ca ratio of the solution (e.g., Katz and Matthews, 1977; Sibley  
204 et al., 1987; 1994; Sibley, 1990), all of which are consistent with a reaction that is  
205 controlled by diffusion through the fluid network. Here, an increase in surface area,  
206 temperature and Mg concentration in solution results in an increase of the net diffusion

207 flux of Mg towards the unreacted calcite crystal and thus the overall reaction rate. Some  
208 experimental studies using powdered material applied an empirical Avrami-type  
209 transformation equation to interpret their rate data, since the reaction progress revealed  
210 the typical S-shaped pattern of Avrami-type transformation curves (Sibley, et al., 1987;  
211 Sibley, 1990). The exponential growth law approximated in Avrami's equation applies  
212 for linear growth and is approximately valid for early stages of diffusion-controlled  
213 growth (Christian, 1975). Diffusion controlled growth as defined by Christian (1975)  
214 refers to the growth of an isolated precipitate particle in a homogeneous medium of  
215 another phase. This is not the case in our experiments and earlier powder experiments.  
216 Thus, the quantitative extrapolation of reaction rates based on powder experiments to  
217 natural systems using an empirical Avrami equation may yield misleading interpretations  
218 with regard to the reaction rate of the overall replacement process.

219         Despite the existence of Avrami-type rate data for carbonate replacement, reactive  
220 transport models on hydrothermal dolomitization in natural systems are often based on  
221 the assumption that the rate of Mg-carbonate precipitation is the rate-limiting step  
222 controlling the replacement of individual crystals. In this case, the formation rate of  
223 dolomite is controlled by three parameters: temperature, surface area and saturation index  
224 (Arvidson and Mackenzie, 1999). The surface area is coupled to the grain size whereas  
225 the saturation index is related to diffusive, dispersive and advective transport of aqueous  
226 species through the fluid network. From our experiments we infer a different quantitative  
227 effect of the texture on the reaction progress and overall rate. The dolomitization rate at a  
228 specific site is strongly grain-size dependent due to different transport distances through  
229 the newly formed polycrystalline rim but also related to 3-D effects of the diffusive flux

230 (note the pronounced reaction rate at the crystal edges visible in the  $\mu$ CT images, see  
231 appendix). The overall rate of dolomitization is then controlled by the supply through the  
232 larger fluid network and the transport through the rim. The spread of the reaction front  
233 and the related reaction rates would differ significantly from the case of a precipitation  
234 rate controlled reaction. Our observations strongly indicate that, for calcite replacement,  
235 the diffusive transport within the pore fluid of the evolving reaction rim is the rate-  
236 limiting step. Our observations and kinetic model provide a better basis to develop a new  
237 parameterization of dolomitization rates that could be used for macroscopic models and  
238 to constrain the temporal and spatial extent of burial dolomitization through highly saline  
239 waters and oilfield brines.

#### 240 **ACKNOWLEDGMENTS**

241 This study was financially supported by German Research Foundation grant  
242 MU2988/2-1 to Müller and Dohmen. Stimulating discussions with John Ferry, Adrian  
243 Immenhauser, Sumit Chakraborty, Andrew Putnis, and Vanessa Helpa are greatly  
244 acknowledged. We thank Shaun Barker and four anonymous reviewers for their  
245 constructive comments, and editor J. Brendan Murphy for the handling of this  
246 manuscript and additional helpful comments.

#### 247 **REFERENCES CITED**

248 Arvidson, R.S., and Mackenzie, F.T., 1999, The dolomite problem: Control of  
249 precipitation kinetics by temperature and saturation state: *American Journal of*  
250 *Science*, v. 299, p. 257–288, doi:10.2475/ajs.299.4.257.

- 251 Bullen, S.B., and Sibley, D.F., 1984, Dolomite selectivity and mimic replacement:  
252 Geology, v. 12, p. 655–658, doi:10.1130/0091-  
253 7613(1984)12<655:DSAMR>2.0.CO;2.
- 254 Christian, J.W., 1975, The theory of transformations in metals and alloys: New York,  
255 Pergamon Press, 1200 p.
- 256 Graf, D.L., and Goldsmith, J.R., 1955, Dolomite-magnesian calcite relations at elevated  
257 temperatures and CO<sub>2</sub> pressures: *Geochimica et Cosmochimica Acta*, v. 7, p. 109–  
258 128, doi:10.1016/0016-7037(55)90023-5.
- 259 Grover, J., and Kubanek, F., 1983, The formation of ordered dolomite from high-  
260 magnesium calcite at 250 °C to 350 °C and 1500 bars: Epitactic growth with optimal  
261 phase orientation, and implications for carbonate diagenesis: *American Journal of*  
262 *Science*, v. 283-A, p. 514–539.
- 263 Jones, G.D., and Xiao, Y., 2005, Dolomitization, anhydrite cementation, and porosity  
264 evolution in a reflux system: Insights from reactive transport models: *AAPG*  
265 *Bulletin*, v. 89, p. 577–601, doi:10.1306/12010404078.
- 266 Kaczmarek, S.E., and Sibley, D.F., 2011, On the evolution of dolomite stoichiometry and  
267 cation order during high temperature synthesis experiments: An alternative model for  
268 the geochemical evolution of natural dolomites: *Sedimentary Geology*, v. 240, p. 30–  
269 40, doi:10.1016/j.sedgeo.2011.07.003.
- 270 Katz, A., and Matthews, A., 1977, The dolomitization of CaCO<sub>3</sub>: An experimental study  
271 at 252 - 295 °C: *Geochimica et Cosmochimica Acta*, v. 41, p. 297–308,  
272 doi:10.1016/0016-7037(77)90238-1.

- 273 Lasaga, A.C., 1986, Metamorphic reaction rate laws and development of isograds:  
274 Mineralogical Magazine, v. 50, p. 359–373, doi:10.1180/minmag.1986.050.357.02.
- 275 Mueller, T., Watson, E.B., and Harrison, T.M., 2010, Applications of Diffusion Data to  
276 High-Temperature Earth Systems, *in* Zhang, Y., and Cherniak, D., eds., Diffusion in  
277 Minerals and Melts: Reviews in Mineralogy and Geochemistry 72, p. 997–1038.
- 278 Perdikouri, C., Kasiopas, A., Geisler, T., Schmidt, B.C., and Putnis, A., 2011,  
279 Experimental study of the aragonite to calcite transition in aqueous solution:  
280 Geochimica et Cosmochimica Acta, v. 75, p. 6211–6224,  
281 doi:10.1016/j.gca.2011.07.045.
- 282 Putnis, A., 2009, Mineral Replacement Reactions: Reviews in Mineralogy and  
283 Geochemistry, v. 70, p. 87–124, doi:10.2138/rmg.2009.70.3.
- 284 Putnis, C.V., Tsukamoto, K., and Nashimura, Y., 2005, Direct observation for  
285 pseudomorphism: Compositional and textural evolution at a solid-fluid interface:  
286 The American Mineralogist, v. 90, p. 1909–1912, doi:10.2138/am.2005.1990.
- 287 Raufaste, C., Jamtveit, B., John, T., Meakin, P., and Dysthe, D.K., 2011, The mechanism  
288 of porosity formation during solvent-mediated phase transformations: Proceedings -  
289 Royal Society. Mathematical, Physical and Engineering Sciences, v. 467, p. 87–124.
- 290 Rosenberg, P.E., Burt, D.M., and Holland, H.D., 1967, Calcite-dolomite-magnesite  
291 stability relations in solutions: The effect of ionic strength: Geochimica et  
292 Cosmochimica Acta, v. 31, p. 391–396, doi:10.1016/0016-7037(67)90049-X.
- 293 Sibley, D.F., 1990, Unstable to stable transformations during dolomitization: The Journal  
294 of Geology, v. 98, p. 739–748, doi:10.1086/629437.

295 Sibley, D.F., Dedoes, R.E., and Bartlett, T.R., 1987, Kinetics of dolomitization: *Geology*,  
296 v. 15, p. 1112–1114, doi:10.1130/0091-7613(1987)15<1112:KOD>2.0.CO;2.

297 Sibley, D.F., Nordeng, S.H., and Borkowski, M.L., 1994, Dolomitization kinetics in  
298 hydrothermal bombs and natural settings: *Journal of Sedimentary Research*, v. 64,  
299 p. 630–637, doi:10.1306/D4267E29-2B26-11D7-8648000102C1865D.

300 Tribble, J.S., Arvidson, R.S., Lane, M., III, and Mackenzie, F.T., 1995, Crystal  
301 chemistry, and thermodynamic and kinetic properties of calcite, dolomite, apatite,  
302 and biogenic silica: Applications to petrologic problems: *Sedimentary Geology*,  
303 v. 95, p. 11–37, doi:10.1016/0037-0738(94)00094-B.

304 Whitaker, F.F., and Xiao, Y., 2010, Reactive transport modeling of early burial  
305 dolomitization of carbonate platforms by geothermal convection: *AAPG Bulletin*,  
306 v. 94, p. 889–917, doi:10.1306/12090909075.

307 Wilson, A.M., Sanford, W., Whitaker, F., and Smart, P., 2001, Spatial patterns of  
308 diagenesis during geothermal circulation in carbonate platforms: *American Journal*  
309 *of Science*, v. 301, p. 727–752, doi:10.2475/ajs.301.8.727.

## 310 **FIGURE CAPTIONS**

311 Figure 1. Backscattered electron image of a polished cross section of a crystal that  
312 reacted for 2 weeks (A) shows that the rim is divided into two layers consisting of  
313 magnesite and dolomite.  $\mu$ CT analysis of a crystal with the same reaction time (B) allows  
314 a three-dimensional reconstruction of the sample. The different layers of the reaction rim  
315 and the unreacted core can be distinguished due to the different X-ray attenuation and  
316 densities of the respective mineral phases.  $\mu$ CT cross sections show that a gap located at  
317 the reaction interface separates the reaction rim from the calcite core.

318

319 Figure 2. A: Fraction of unreacted calcite and fraction transformed to magnesite and  
320 dolomite as a function of time. Both the fraction of unreacted calcite and the total fraction  
321 transformed as a function of time follow an exponential trend ( $R^2 = 0.98$ ). The total  
322 fraction transformed  $\zeta$  (B) and the Ca/Mg ratio of the reacted fluid (C) can be fitted with  
323 a square root of time relation.

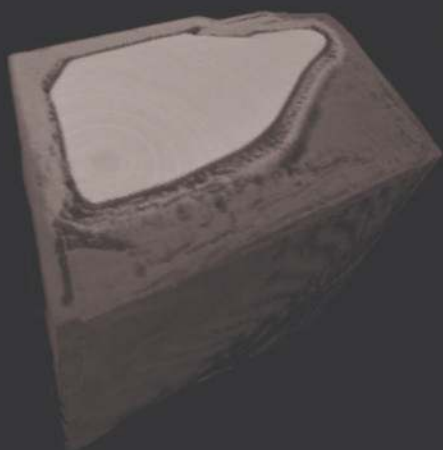
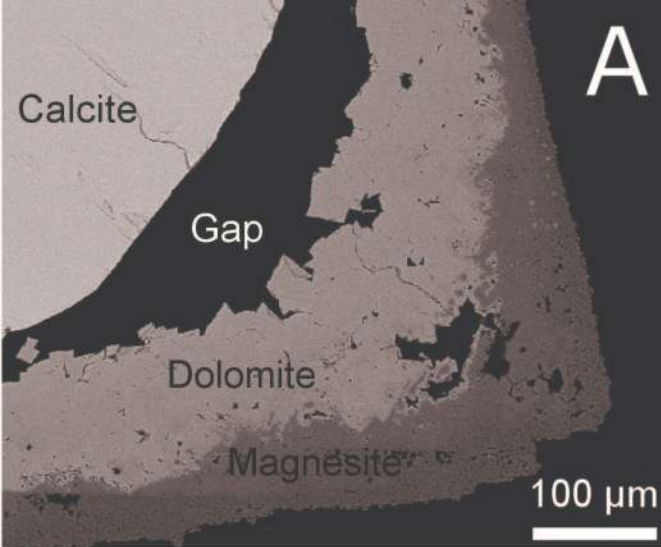
324

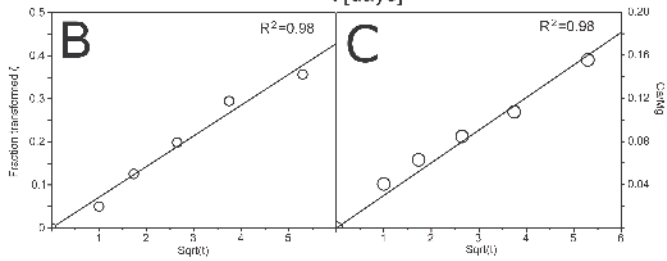
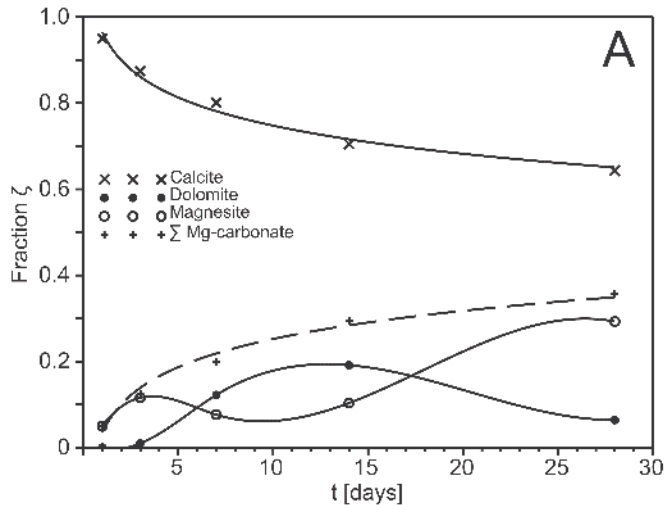
325 Figure 3. A: The growth of the reaction front depends on the flux of the relevant aqueous  
326 species ( $J_{Mg^{2+}}$ ,  $J_{Ca^{2+}}$ ,  $J_{CO_3^{2-}}$ ) in the fluid and is accompanied by a considerable molar  
327 volume change ( $\Delta V$ ). B: The fluid composition in the rim changes with time. In early  
328 stages of the reaction, the ion activity product (IAP) of magnesite in the interfacial fluid  
329 exceeds the equilibrium solubility product (K) of magnesite, i.e., the saturation index  
330  $[SI = -\log(\frac{IAP}{K})]$  with respect to magnesite at the interface is  $>0$  and magnesite  
331 precipitates (stage 1). After 7 days, the Ca-concentration at the interface increases and the  
332 SI of dolomite is reached (stage 2). In the final stages, the Mg-concentration at the  
333 interface increases, and the fluid becomes supersaturated with respect to magnesite (stage  
334 3).

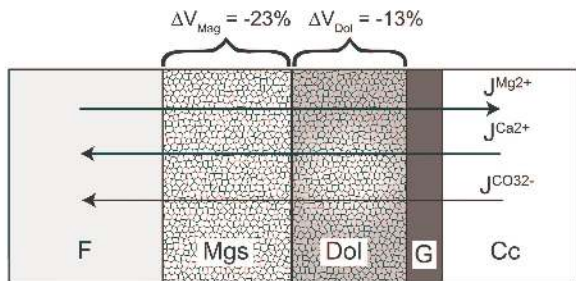
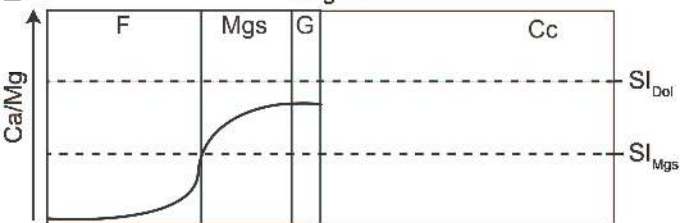
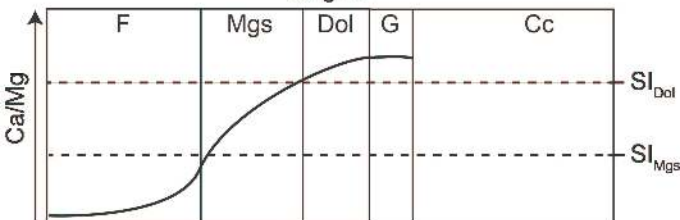
335

336 <sup>1</sup>GSA Data Repository item 2015xxx, xxxxxxxx, is available online at  
337 [www.geosociety.org/pubs/ft2015.htm](http://www.geosociety.org/pubs/ft2015.htm), or on request from [editing@geosociety.org](mailto:editing@geosociety.org) or  
338 Documents Secretary, GSA, P.O. Box 9140, Boulder, CO 80301, USA.







**A****B****Stage 1****Stage 2****Stage 3**